

Photoexcitation dynamics in regioregular and regiorandom polythiophene films

O. J. Korovyanko, R. Österbacka,* X. M. Jiang, and Z. V. Vardeny
Department of Physics, University of Utah, Salt Lake City, Utah 84112

R. A. J. Janssen

Laboratory of Macromolecular and Organic Chemistry, Eindhoven University of Technology, 5600 MB Eindhoven, The Netherlands
(Received 24 August 2001; published 28 November 2001)

Using a variety of optical probes techniques we studied the photoexcitation dynamics in thin films of poly-3-hexyl thiophene with regioregular order that forms lamellae structures with increased interchain interaction, as well as regiorandom order that keeps a chainlike morphology. In regiorandom films we found that intrachain excitons with correlated induced absorption and stimulated emission bands are the primary excitations; they give rise to a moderately strong photoluminescence band. In regioregular films, on the contrary, we found that the primary excitations are excitons with a much larger interchain component; this results in lack of stimulated emission, vanishing intersystem crossing, and very weak photoluminescence band. In regioregular films we also measured photogenerated geminate polaron pairs with ultrafast dynamics that are precursor to long-lived polaron excitations.

DOI: 10.1103/PhysRevB.64.235122

PACS number(s): 78.30.Jw, 78.47.+p, 78.55.Kz

Interest in π -conjugated polymers (PCP's) has recently soared due to the potential optoelectronic applications including light-emitting diodes, solar cells, and field-effect transistors. The interest in PCP's has recently attracted the Nobel Prize in Chemistry that was given to Heeger, McDiarmid, and Shirakawa in December 2000. For many of the optoelectronic applications, the degree of structural order of the PCP active layer has been recognized as one of the key parameters governing the photophysics and consequently also its specific application for the optimal device performance. Whereas interchain interactions are usually detrimental for the PCP use in light-emitting diodes due to weak optical coupling to the ground state,¹ charge transport in the other applications requires good contacts between neighboring conjugated chains in the film. In addition, the traditional one-dimensional (1D) electronic structure in PCP's results in strong self-localization of the electronic excitations, which may also limit the carrier mobility to values of the order of 10^{-4} cm²/V sec.²

Much higher mobilities, of the order of 0.1 cm²/V sec have been recently obtained with regioregular substituted poly-3-hexyl thiophene (RR-P3HT) [see Fig. 1(b) inset] in field-effect transistors (FET's).³ Such films were also successfully used in a FET device to drive a light emitting diode based on PCP that demonstrated an all-organic display pixel.⁴ Moreover, semiconductor to metal transition as well as superconductivity at a temperature of about 2.5 K have been recently demonstrated with RR-P3HT FET's, where the carriers were injected into a thin polymer layer below the gate electrode.⁵ The reason for the dramatic increase in carrier mobilities is that self-organization of RR-P3HT chains results in a lamellae structure perpendicular to the film substrate.³ In such lamellae two-dimensional (2D) sheets are formed having strong interchain interaction due to the short interchain interlayer distance of the order of 3.8 Å. Delocalization of the charge carrier has been invoked to be the reason for the high interlayer mobility. Recent optical studies of RR-P3HT films, where delocalized polaron excitations on

adjacent chains have been measured using charge induced optical techniques in FET's,^{3,6} as well as direct photogeneration in thin films,⁷ have confirmed this assumption. On the contrary, P3HT films casted from polymer chains having regiorandom (RRa-) order [see Fig. 1(a) inset] form ordered lamellae to a much lesser extent and the obtained field-effect

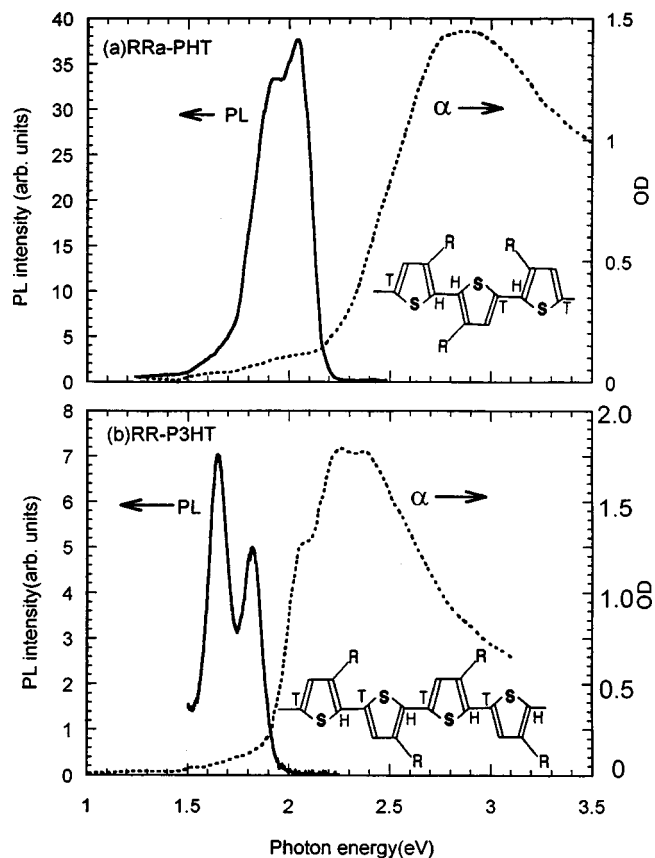


FIG. 1. The room-temperature absorption and photoluminescence spectra of RRa-P3HT (a) and RR-P3HT (b) films. The respective polymer regio-order structures are given in the insets.

carrier mobilities in FET's are consequently small.³ The main reason for the reduced carrier mobility is the lack of sufficiently strong interchain interaction that is caused by the chainlike film morphology. The effect of the strong interchain interaction on the *neutral* excitations in P3HT films should be quite interesting.¹ However, to this date studies focused on the *neutral* excitations in P3HT films of various regio-orders have not been reported.

In this work we study the photoexcitation dynamics in films of RR-P3HT and compare them to those obtained in films of RRA-P3HT. For these studies we have used a variety of steady-state and transient optical techniques covering the time domains from femtoseconds (fs) to 200 picoseconds (ps), as well as photomodulation and magneto-optical measurements under steady-state conditions. We found that the photoexcitations in RRA-P3HT films are similar in many respects to those found in other luminescent PCP films.^{8–12} The primary excitations in the ps time domain are intrachain excitons with correlated photoinduced absorption (PA) and nonoverlapping stimulated emission (SE) bands. At longer times we identified long-lived triplet excitons with a near-infrared PA band, which are formed via intersystem crossing to the triplet manifold that competes with the moderately strong (8% quantum efficiency) photoluminescence (PL) band. On the contrary, we found in lamellae RR-P3HT films that the primary excitations are excitons with much larger interchain contribution. This leads to a weaker optical transition to the ground state that results in much weaker PL (<0.5%), lack of SE, and also to a vanishing intersystem crossing that gives rise to no triplets. In addition we also identified the precursor to polaron photogeneration in these films; these are geminate polaron pairs with ultrafast dynamics.

The optical studies were performed using both ps transient and cw techniques. The time-resolved technique was the pump-probe correlation with 100 fs time resolution and spectral range from 1.1 to 2.2 eV, whereas the cw techniques include absorption, emission, PA and PA-detected magnetic resonance (PADMR) spectroscopies, in the spectral range from 0.3 to 3.5 eV.

In the ps time-resolved measurements the short pump pulse creates photoexcitations in the film and a time-delayed probe pulse measures the resulting change in transmission as a function of the pump-probe delay time (achieved by moving a translation stage). We used pulses from an amplified Ti:sapphire laser system operating at a repetition rate of 1 kHz. Pulses 50 fs in duration centered at 800 nm were doubled into the UV (400 nm, or 3.1 eV) using second harmonic generation in a BBO crystal. Probe pulses of variable wavelength were produced by using a portion of the amplified 800-nm beam to generate a femtosecond white light supercontinuum in a 1-mm-thick sapphire plate. An overall time resolution of ~ 90 fs in the pump-probe measurements was achieved by adjusting the stage to compensate the spectral chirp as measured by time-resolved two-photon absorption in DOO-PPV.¹³ Wavelength resolution of about 6 nm in the probe beam was achieved by a 0.3 m monochromator having a 200- μ m exit slit, that was placed in the probe beam after it had passed through the film. The pump beam was modulated

mechanically at exactly half the repetition rate of the Ti:sapphire laser system (≈ 500 Hz),¹⁴ and the resulting change, ΔI in the probe beam energy, I was detected with phase sensitive technique using lock-in amplification. For the purpose of noise reduction, a separate reference beam was split off from the probe beam prior to its interaction with the pump beam on the sample. The reference beam passed the sample at a different spot and was also dispersed with the same monochromator prior to detection by a separate, matched Si photodiode. To correct the pump-probe signal for intensity fluctuations in the supercontinuum at the selected probe wavelength, the probe signal was normalized by the reference signal at each delay time point (this technique was dubbed before as “A-B”¹⁴) with a significant improvement in the measurements sensitivity of up to $\Delta I/I \approx 10^{-4}$.

For the present studies all measurements were carried out at room temperature in a cryostat providing a dynamical vacuum of 100 μ Torr to prevent the polymer degradation with strong laser illumination at ambient conditions.¹⁵ Pump-probe signals were measured over a range of pump intensities to ensure linearity of the response with respect to the initial photoexcitation density; we thus work at intensities below 300 μ J/cm² per pulse to prevent signal saturation. Since the photoexcitation dynamics depend on the excitation density, care was taken in the experimental design to minimize distortion of the measured pump-probe response by spatial inhomogeneity of the photoexcitation distribution. The pump beam was focused onto the sample to a 1-mm-diameter round spot, whereas the probe beam was focused using an achromatic lens onto a 0.3-mm-diameter spot in the center of the pump illuminated spot. To ensure the reproducibility of the alignment, the spatial overlap of the pump-probe beams was set using a telescopic microscope.

For the ps transient measurements we used the time-resolved differential transmittance technique with time delays ranging from 100 fs to 200 ps. For each sample film, measurements were carried out over a range of pump fluences that correspond to a range of initial photoexcitation densities from 5×10^{17} to 5×10^{19} cm⁻³. Photoexcitations resulted in PA, which is represented in the spectra as negative differential transmittance, $-\Delta T/T$, where ΔT is the change in transmittance, T due to the action of the pump pulse. Since the pump and probe beams are linearly polarized we could measure ΔT_{pa} (ΔT_{pe}), where the pump and probe polarization are parallel (perpendicular) to each other. Pump induced SE and photobleaching (PB) of the optical absorption in the ground state with $\Delta T > 0$ were also measured. In the small signal limit, $\Delta T(t)$ is expected to be proportional to the photoexcitation density $N(t)$, which for an optically thick film is given by the relation $\Delta T/T = N\sigma/\alpha_L$, where σ is the photoexcitation optical cross section of and α_L is the absorption coefficient at the laser excitation wavelength.

For the cw PA measurements we used a standard photomodulation setup at 10 K.¹⁶ In this technique $\Delta T/T$ spectrum is measured in a much broader spectral range using a number of solid-state detectors, a lock-in amplifier referenced to a modulated cw Ar⁺ laser beam used for excitation, and a dispersed beam from an incandescent light source as a probe. The PL spectrum is recorded without the probe beam on the

sample, in order to eliminate pump-related emission to interface with the ΔT measurements. Also we used a calibrated integrated sphere to determine the absolute PL quantum efficiency in the films. The cw PA technique is sensitive to long-lived photoexcitations having lifetime of the order of $1/f$, where f is the pump beam modulation. Usually a variety of photoexcitations contribute to $\Delta T/T$ spectrum and we have to use other means to separate their contributions in the PA spectrum.

We have applied the PADMR spectroscopy¹⁶ to separate the various photoexcitations contributions according to their spin-related recombination kinetics. This is usually related to the photoexcitations spin state. In this way we could separate spin-1 from spin- $\frac{1}{2}$, and spin-0 photoexcitations in the PA spectra. For the PADMR spectroscopy¹⁶ the sample was mounted in a high- Q microwave cavity at 3 GHz equipped with a superconducting magnet and illuminated by the cw pump and probe beams and the microwaves. We measured the H -PADMR spectrum, in which δT is monitored at a fixed probe wavelength λ as the magnetic field H is varied, as well as the λ -PADMR spectrum where δT is measured at a fixed magnetic field, while the probe beam is varied.

The samples were thin films of RR-P3HT (92% RR regio-order, M_w of 28 kg/mol) that were grown in our laboratory as well as RR-P3HT and RRa-P3HT that were purchased from Aldrich.¹⁷ The films were cast from chloroform or xylene solutions (usually at a concentration of a few mg/ml) onto sapphire or quartz substrates. Special care was taken to minimize contamination of the powders and films by oxygen and water at ambient conditions.

Figure 1 shows the absorption and PL spectra of RRa-P3HT and RR-P3HT films at room temperature. The strong absorption band over the gap is due to π - π^* transitions, and according to Kasha's rule, the PL emission comes from the lowest exciton in the system. We note the redshift of the RR-P3HT absorption and PL bands with respect to those in RRa-P3HT which is caused by the superior order in the lamellae.³ The planar order leads to polymer chains with longer conjugations that are due to fewer defects, such as twists and radicals on the chains. In addition, the absorption and the PL bands of the RR-P3HT film show pronounced structures due to phonon replica, indicating that the polymer chains in this film are more homogeneous than those in RR-P3HT films. In spite of the superior order, we measured in RR-P3HT an order of magnitude decrease in the PL quantum efficiency η , in RRa-P3HT we measured $\eta \approx 8\%$, whereas in RR-P3HT we measured $\eta < 0.5\%$. The η decrease in RR-P3HT cannot be explained by an increase in the nonradiative decay rate, because this film contains fewer defects and intersystem crossing to the triplet manifold is absent (see below). We conjecture therefore that η decrease in RR-P3HT is due to a weaker radiative transition of the lowest lying excitons in this film. A similar conclusion was reached for the excitons in RR-P3HT chains that form aggregates when dissolved in poor solvents.¹⁸ The weaker optical transition may be due to a larger interchain contribution for the lowest excitons in the lamellae, compared to the usual intrachain excitons in RRa-P3HT. Indeed an interlayer separation of 3.8 Å in RR-P3HT lamellae causes a stronger interchain-

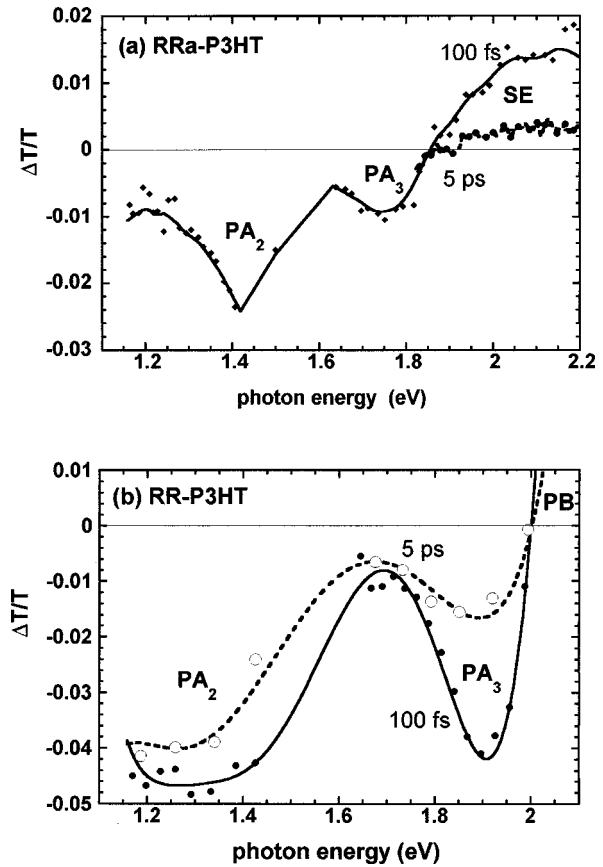


FIG. 2. The transient PA spectra of RRa-P3HT (a) and RR-P3HT (b) measured at 100 fs (full diamonds and circles) and 5 ps (full and empty circles), respectively, following the pulse excitation. The PA, SE, and PB bands are assigned.

interlayer interaction, as recently calculated using numerical quantum-chemical methods.^{1,19} For an H -aggregate chain configuration this interaction leads to splitting of the HOMO and LUMO levels, so that the lower, redshifted LUMO level becomes optically forbidden.¹ The weak PL that is still detected in RR-P3HT may be due to defects that are present in the film, which relax the optical selection rules. This model may explain the weak PL in RR-P3HT, as well as its redshift. The higher splitted LUMO level is optically allowed in this model,¹ and may be directly seen in absorption, which should be blue shifted with respect to the PL. Hence from the Stokes shift of the 0-0 transition in absorption and PL spectra [Fig. 1(b)] we obtain an upper limit for the LUMO splitting in RR-P3HT of 250 meV,²⁰ in good agreement with recent model calculations.^{1,19}

The ps dynamics studies in P3HT may further elucidate the excitons characteristic properties. Figure 2 shows the transient PA spectra of P3HT with both regio-orders measured at $t = 100$ fs and $t = 5$ ps, respectively, following the pulse excitation. The transient PA spectra of both films show two PA bands (PA₂ and PA₃), but only the fs spectrum of RRa-P3HT contains a SE band that is due to the photogenerated excitons. We explain the lack of SE in RR-P3HT as due to the much smaller oscillator strength for the photogenerated excitons in this material, confirming the above conclusion that the lowest lying excitons in RR-P3HT films are, in fact, optically forbidden.

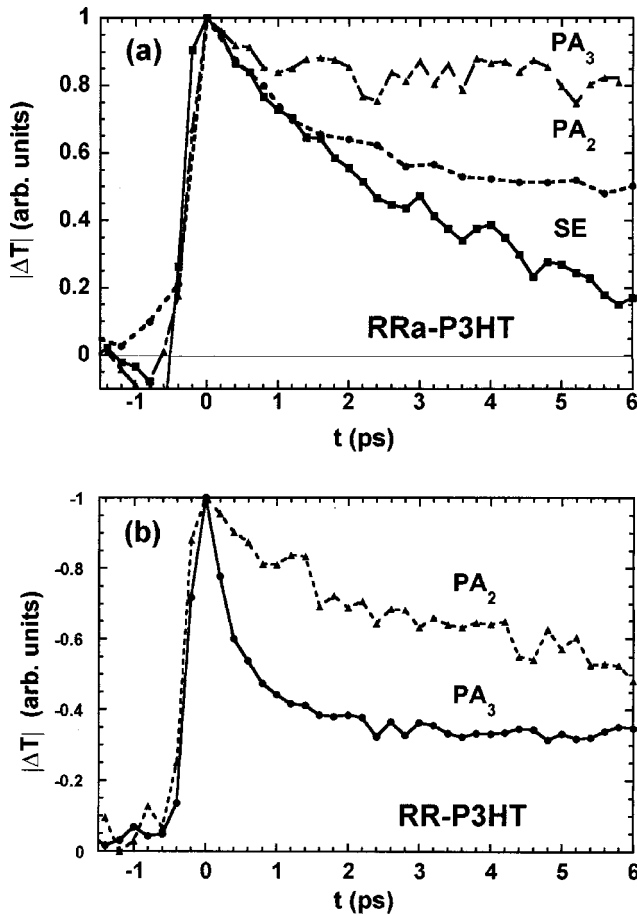


FIG. 3. Transient PA and SE decays in RRa-P3HT (a) and RR-P3HT (b), up to 6 ps.

To better characterize the primary excitations in RRa-P3HT that are revealed in the ultrafast PA spectra, we studied the transient dynamics of each PA band and compared it with that of the SE band. Figure 3(a) shows that the dynamics of PA₂ is similar to that of SE; both bands initially decay together, but the SE band disappears from the spectrum at 15 ps [Fig. 2(a)] that is caused by the competing effect of PA₃. Due to their correlated dynamics at several different excitation intensities we conjecture that PA₂ and SE belong to the same species, namely intrachain excitons. A similar conclusion was drawn before for the correlated excitonic PA and SE in other PCP films.^{8–12} Moreover, in some of the previous studies,^{8,21} another correlated PA band (PA₁) was detected in the near infrared (IR) spectral range and was also assigned to photogenerated excitons. In view of this, we anticipate that another excitonic PA band exists in RR-P3HT in the near IR spectral range; this, however, will be confirmed in future studies.

On the contrary, PA₃ decay in RRa-P3HT is much slower than that of SE and PA₂ [Fig. 3(a)] and therefore it does not involve intrachain excitons. In fact, it decays only by a factor of about 2 from its initial $t=0$ value within the maximum time delay of our apparatus (200 ps). We conjecture, therefore that PA₃ is due to interchain, trapped polaron pairs. A similar conclusion was drawn previously in ps studies of other PCP films.^{9–11} Such excitations may also be instantane-

ously generated onto two adjacent chains at a place on the chains close to their “contact point,” where the interchain distance is the smallest. Actually, contact points may be also formed on the same chain between different chain segments, due to the chain molecular “cylindrical conformation” recently found in MEH-PPV using polarized PL.²² This may explain the recent ps PA studies in some PPV-based PCP films, which were conducted in the mid-IR spectral range (8–12 μm), where instantaneously generated infrared active vibrations (IRAV’s) were detected.^{23,24} From this it was conjectured²⁴ that separated polarons are the primary excitations in PCP films. In view of our present results it is clear that in PCP films simultaneously with intrachain excitons, polaron pairs on adjacent chains or neighboring chain segments may be also generated. If the polarons reside on different chains or different segments of the same chain, then the polaron pair species can also give rise to IRAV’s. However, as a result of the Coulomb attraction between the oppositely charged polarons, the polaron pair species are trapped near the contact point of the adjacent chains (or neighboring segments) at which they had been originally generated. The slow dynamics of the polaron pair species may also be obtained via the decay of the polarization memory, $P(t) = (\Delta T_{\text{pa}} - \Delta T_{\text{pe}}) / (\Delta T_{\text{pa}} + \Delta T_{\text{pe}})$, where ΔT_{pa} (ΔT_{pe}) is the PA measured with pump and probe polarization parallel (perpendicular) to each other. Indeed, we measured a long-lived $P(t)$ for the PA₃ band, which is much longer than that of PA₂.

We studied the PA dynamics of the two PA bands also in RR-P3HT films [Fig. 3(b)]. As in RRa-P3HT we also found that the ps transient decays of PA₂ and PA₃ in this film are not correlated. Moreover the decay dynamics of PA₂ depends on the excitation intensity I showing faster decay at higher I [Fig. 4(a)] that is perhaps due to exciton-exciton annihilation,²⁵ whereas the decay dynamics of PA₃ is independent on I [Fig. 4(b)]. From this and the similarity with the PA transient spectrum in RRa-P3HT discussed above, we conclude that PA₂ and PA₃ in RR-P3HT are likewise due to excitons and geminate polaron pairs, respectively. The lack of ps SE band in RR-P3HT shows that the excitons in the lamellae are not regular intrachain excitons. This may explain the reason why the excitonic PA band in this film, namely PA₂ [Fig. 2(b)] is much broader than that in RRa-P3HT [Fig. 2(a)]. The observed broadening may be due to the splitting of the even parity states (A_g) that are optically coupled to the lower lying excitons (or “ $1B_u$ ”). Similar as for the LUMO level¹ these A_g states may also split due to the increased interlayer interchain coupling in the lamellae causing excess broadening to their optical transitions.

The band PA₃ in RR-P3HT [Fig. 2(b)] is substantially stronger than that in RRa-P3HT [Fig. 2(a)]. This shows that polaron pair generation is more efficient in RR-P3HT films. This is not surprising since the polymer chains in the lamellae are longer and closer to each other, so that the contact points between any two adjacent chains are therefore more extended. Moreover, the extended contact points for the polymer chains in the lamellae leads to a more mobile polaron pair species in RR-P3HT compared to that in RRa-P3HT. This results in a faster PA₃ decay [Fig. 4(b)]

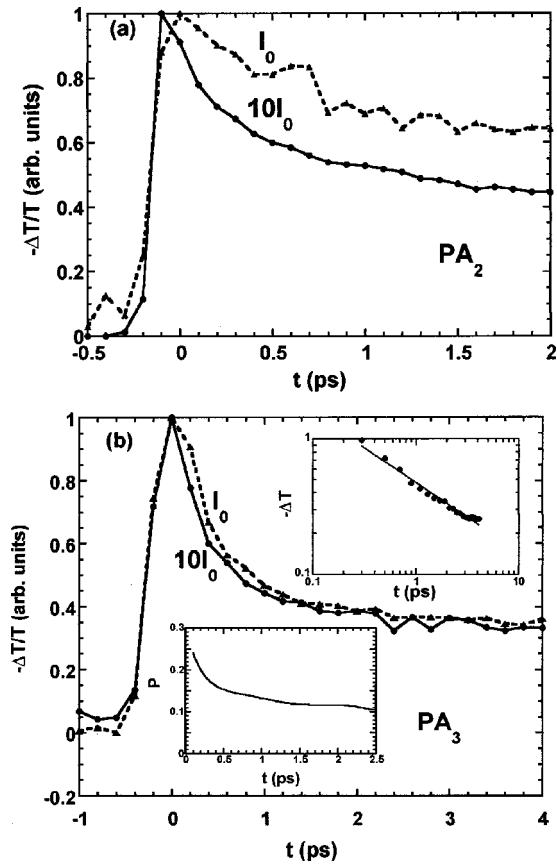


FIG. 4. Transient decays of PA₂ (a) and PA₃ (b) bands in RR-P3HT at two different excitation intensities of I_0 of $20 \mu\text{J}/\text{cm}^2$ and $10I_0$ (or $200 \mu\text{J}/\text{cm}^2$), respectively. The upper inset in (b) shows the PA₃ decay in logarithmic scale and a power-law fit to the data, whereas the lower inset shows its polarization memory decay $P(t)$.

inset] in RR-P3HT compared to that in RRa-P3HT [Fig. 3(a)]. We could fit PA₃ transient decay in RR-P3HT with a two-component decay function; a fast component using a $t^{-1/2}$ decay with a 0.5-ps lifetime [Fig. 4(b) inset], and a slow component. The $t^{-1/2}$ decay that we found for the geminate polaron pair in RR-P3HT is in agreement with the diffusion-limited geminate recombination considered before for the photogenerated geminate soliton-antisoliton pair recombination in t -(CH)_x.²⁶ Similar as in RRa-P3HT, the slow PA₃ component in RR-P3HT decays only slightly during the 200-ps time interval of our measurements. We interpret the two PA₃ decay components as polaron pairs that are generated in the lamellae, which are more mobile and consequently have faster dynamics, and polaron pairs that are generated in the disordered portions of the polymer film. The latter, similarly as in RRa-P3HT are less mobile and consequently have slower dynamics. This two-component dynamics is also apparent in $P(t)$ decay obtained at probe energies within the PA₃ band [Fig. 4(b) inset]. We found that $P(t)$ quickly decays to a plateau level within about 1 ps, similar to the PA₃ fast component decay. This shows that the fast PA₃ component belongs to the more mobile species, such as polaron pairs in the lamellae; its spectrum, however, is indistinguishable from that of polaron pairs in the disordered portion of the film.

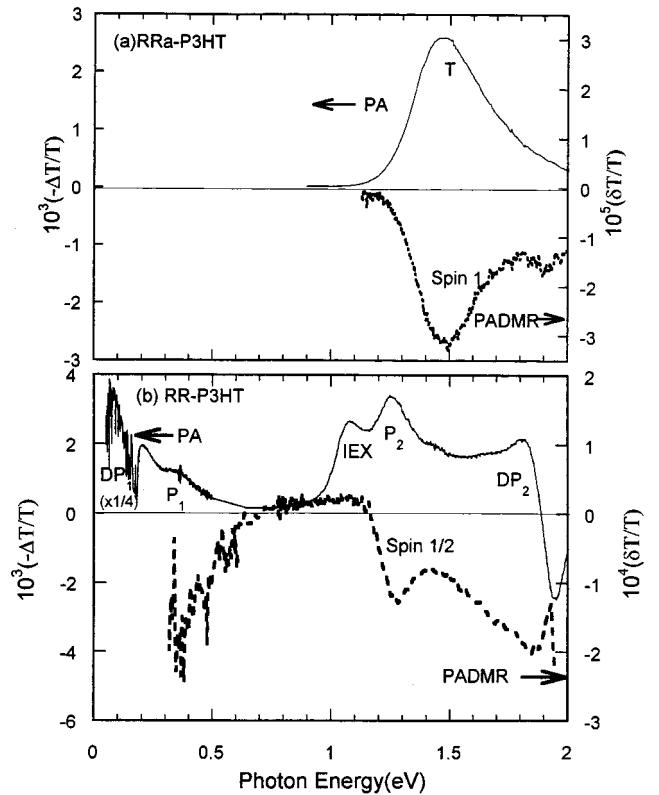


FIG. 5. Cw PA and λ -PADMR spectra of RRa-P3HT (a) and RR-P3HT (b) films measured at 10 K. The λ -PADMR in (a) was measured at $H_{1/2}=430$ G, which corresponds to transitions among spin-1 triplet sublevels at $g \approx 5.1$, whereas in (b) it was measured at $H=1006$ G, which corresponds to transitions among spin- $\frac{1}{2}$ doublet sublevels at $g \approx 2$. Several PA bands are assigned.

The *long-lived* photoexcitations in the P3HT films were studied by cw PA and PADMR spectroscopies. Figure 5(a) shows that a single PA band, T at 1.45 eV dominates the spectrum in RRa-P3HT. We also found that λ -PADMR measured at resonant magnetic field, $H_{1/2}=430$ G corresponding to $g \approx 5.1$, which is due to microwave transitions between two triplet sublevels with a substantial zero-field splitting (dubbed “half field”²⁷), is similar to the PA spectrum. This unambiguously shows that T band is due to triplet excitons. The long-lived triplets are formed via intersystem crossing to the triplet manifold with a time constant longer than our ps measurements limit of 200 ps. In fact, typical intersystem crossing time in PCP films were determined to be of the order of 5 ns.⁸ This long decay time would not be seen in our ps transient measurements.

The cw PA spectrum in RR-P3HT is much richer.⁷ It contains two PA bands DP₁ at 0.1 eV and DP₂ at 1.85 eV, respectively that are due to 2D delocalized polarons in the lamellae,^{3,6-7} as well as PA bands P₁ at 0.35 eV and P₂ at 1.25 eV, respectively, that are due to localized polarons in the disordered portions of the film.⁷ In addition, the PA spectrum also contains a PA band IEX at 1.1 eV that was tentatively identified²⁷ as due to trapped interchain singlet excitons in the lamellae. The λ -PADMR spectrum measured in RR-P3HT at resonant field that corresponds to $g \approx 2$ due to spin- $\frac{1}{2}$ carriers is shown in Fig. 5(b) and confirms the previous PA

assignments. This spectrum shows that, except for the IEX band, all other PA bands in the spectrum are associated with spin- $\frac{1}{2}$ carriers. In particular DP₂, which spectrally overlaps with PA₃ in the ps transient spectrum [Fig. 2(b)], may be associated with polarons. This may indicate that PA₃ in RR-P3HT is a precursor to the formation of long-lived polarons in the film, in agreement with its assignment in the transient spectra above. In fact the band DP₂ may be due to the long-lived tail of the species associated with PA₃ in the ps time domain. It is also seen in Fig. 5(b) that IEX is not associated with any spin- $\frac{1}{2}$ excitation, in agreement with its previous assignment²⁸ that it is due to trapped spin *singlet* excitons. We note that IEX spectrally overlaps with PA₂ [Fig. 2(b)] indicating that these two bands, in fact, belong to the same species; except that the IEX represents the long-lived tail of the photogenerated excitons associated with PA₃.

Using PADMR at $H_{1/2}$ as in RR-P3HT [Fig. 5(a)], long-lived spin-1 excitations *have not* been found in the lamellae. This shows that long-lived triplet excitons are not easily generated in RR-P3HT films. In RR-P3HT solutions, on the contrary, long-lived photogenerated triplets do exist, and an intersystem crossing (ISC) time constant of about 5 ns was determined.²⁹ We therefore conjecture that the delocalized interchain interlayer excitons in the lamellae do not easily turn into localized intrachain triplet excitons in RR-P3HT via ISC. This is another strong evidence that the primary excitations in RR-P3HT are not intrachain excitons as found in

many other PCP films. Instead, they are delocalized among adjacent layers similar to the delocalized polarons in the lamellae studied before,^{3,6-7} with a consequent suppression of ISC into the triplet manifold. We note that ISC suppression was also observed recently in aggregates of long oligothiophenes below the aggregate formation temperature.³⁰ ISC suppression might therefore be a general consequence of enhanced interchain interaction.

In conclusion, we studied and compared the primary and long-lived photoexcitations in P3HT films with two different regio-orders, RR-P3HT with lamellae structure and RRA-P3HT with chainlike morphology. We found that, similar to other PCP films, the primary excitations in P3HT are excitons and polaron pairs. However, the excitons in RR-P3HT are delocalized among adjacent chains in different lamellae, acquiring a large interchain component. This leads in RR-P3HT to lack of stimulated emission, weak PL emission, and vanishing triplet excitons that are generated via ISC. The delocalized excitons in RR-P3HT films that we found here in fact complement the delocalized polaron excitations that were previously observed in the lamellae films.

The work at the University of Utah was supported in part by the NSF DMR 97-32820 and DOE ER-45490. R.O. acknowledges funding from the Swedish Academy of Engineering Sciences in Finland, the Neste Ltd. Foundation, and the Ehrnrooth Foundation.

*Present address: Department of Physics, Åbo Akademi University, Porthansgatan 3, FIN-20500 Turku, Finland.

¹J. Cornil, D. Beljonne, J. P. Calbert, and J. L. Bredas, *Adv. Mater.* **13**, 1053 (2001).

²G. Horowitz, *Adv. Mater.* **10**, 365 (1998).

³H. Sirringhaus *et al.*, *Nature (London)* **401**, 685 (1999).

⁴H. Sirringhaus, N. Tessler, and R. H. Friend, *Science* **280**, 1741 (1998).

⁵J. H. Schon, A. Dodabalapur, Z. Bao, C. Kloc, and B. Batlogg, *Nature (London)* **410**, 189 (2001).

⁶P. J. Brown, H. Sirringhaus, M. Harrison, M. Shkunov, and R. H. Friend, *Phys. Rev. B* **63**, 125204 (2001).

⁷R. Österbacka, C. P. An, X. M. Jiang, and Z. V. Vardeny, *Science* **287**, 839 (2000).

⁸S. V. Frolov *et al.*, *Phys. Rev. Lett.* **78**, 4285 (1997).

⁹V. I. Klimov, D. W. McBranch, N. Barashkov, and J. Ferraris, *Phys. Rev. B* **58**, 7654 (1998).

¹⁰C. Silva *et al.*, *Chem. Phys. Lett.* **23**, 277 (1998); M. A. Stevens, C. Silva, D. M. Russell, and R. H. Friend, *Phys. Rev. B* **63**, 165213 (2001).

¹¹B. Kraabel *et al.*, *Phys. Rev. B* **61**, 8501 (2000).

¹²A. Dogariu, A. J. Heeger, and H. Wang, *Phys. Rev. B* **61**, 16 183 (2000).

¹³O. J. Korovyanko, G. A. Levina, and Z. V. Vardeny, *Synth. Met.* **119**, 631 (2001).

¹⁴V. I. Klimov and D. W. McBranch, *Opt. Lett.* **23**, 277 (1998).

¹⁵M. Yan *et al.*, *Phys. Rev. Lett.* **72**, 1104 (1994); **75**, 1992 (1995).

¹⁶Z. V. Vardeny and X. Wei, in *Handbook of Conducting Polymers*,

edited by T. A. Skotheim, R. Elsenbaumer, and J. R. Reynolds, 2nd edition (Dekker, New York, 1997).

¹⁷Aldrich Chemical Company, Milwaukee, Wisconsin.

¹⁸G. Rumbles *et al.*, *Synth. Met.* **101**, 158 (1999).

¹⁹D. Beljonne *et al.*, *Adv. Funct. Mater.* **11**, 1 (2001).

²⁰Other mechanisms, such as exciton migration to the longest chain outside the lamellae structures, may also contribute to the apparent PL Stokes shift.

²¹S. V. Frolov, Z. Bao, M. Wohlgenannt, and Z. V. Vardeny, *Phys. Rev. Lett.* **85**, 2196 (2000).

²²D. Hu, J. Yu, K. Wong, B. Bagchi, P. J. Rossky, and P. F. Barbara, *Nature (London)* **405**, 1030 (2000).

²³U. Mizrahi, D. Gershoni, E. Ehrenfreund, and Z. V. Vardeny, *Synth. Met.* **102**, 1182 (1999); *ibid.* **119**, 507 (2001).

²⁴D. Moses, A. Dogariu, and A. J. Heeger, *Chem. Phys. Lett.* **316**, 354 (2000); *Phys. Rev. B* **61**, 9373 (2000).

²⁵A. Dogariu, D. Vacar, and A. J. Heeger, *Phys. Rev. B* **58**, 10 218 (1998), and references therein.

²⁶Z. V. Vardeny *et al.*, *Phys. Rev. Lett.* **49**, 1657 (1982); C. Shank *et al.*, *ibid.* **49**, 1660 (1982).

²⁷R. Österbacka, M. Wohlgenannt, D. Chinn, and Z. V. Vardeny, *Phys. Rev. B* **60**, R11 253 (1999).

²⁸R. Österbacka, C. P. An, X. M. Jiang, and Z. V. Vardeny, *Synth. Met.* **116**, 317 (2001).

²⁹B. Kraabel, D. Moses, and A. J. Heeger, *J. Chem. Phys.* **103**, 5102 (1995).

³⁰J. J. Apperloo, R. A. J. Janssen, P. R. L. Malenfant, and J. M. J. Frechet, *J. Am. Chem. Soc.* **123**, 6916 (2001).